





Lightweight Curvature Estimation on Point Clouds with Randomized Corrected Curvature Measures Supplementary material

J.-O. Lachaud¹  and D. Coeurjolly²  and C. Labart¹ and P. Romon³  and B. Thibert⁴ 

¹Université Savoie Mont Blanc, France

²Univ Lyon, CNRS, INSA Lyon, UCBL, LIRIS UMR5205, France

³Université Gustave Eiffel, France

⁴Université Grenoble Alpes, France

1. Study of error laws induced by perturbations in normal and position

Recalling notations. Let $\hat{\mathbf{q}}$ be a point of interest (e.g. some $\hat{\mathbf{x}} \in X$) and let \mathbf{q} be its projection on S . Let $(\hat{\mathbf{x}}_i)_{i \in I}$ be the points in the ball centered on $\hat{\mathbf{q}}$ and of radius $\delta/2$, with $I \subset \{1, \dots, N\}$. Let $(\hat{\tau}_l)_{l=1 \dots L}$ be L triangles with vertices in $(\hat{\mathbf{x}}_i)_{i \in I}$. Order of vertices within triangle $\hat{\tau}_l$ is chosen so as $\mu_{\hat{\mathbf{u}}}^{(0)}(\hat{\tau}_l)$ is a non-negative number. To each triangle $\hat{\tau}_l$ corresponds an unperturbed triangle τ_l with vertices on the surface S .

Let $\hat{A}^{(0)} := \sum_{l=1}^L \mu_{\hat{\mathbf{u}}}^{(0)}(\hat{\tau}_l)$, $A^{(0)} := \sum_{l=1}^L \mu_{\mathbf{u}}^{(0)}(\tau_l)$, $\hat{A}^{(1)} := \sum_{l=1}^L \mu_{\hat{\mathbf{u}}}^{(1)}(\hat{\tau}_l)$, $A^{(1)} := \sum_{l=1}^L \mu_{\mathbf{u}}^{(1)}(\tau_l)$. Finally, let us define $\bar{Z}_L^{(0)} := \frac{1}{L}(\hat{A}^{(0)} - A^{(0)})$ and $\bar{Z}_L^{(1)} := \frac{1}{L}(\hat{A}^{(1)} - A^{(1)})$, which are respectively the error laws in area and mean curvature induced by data perturbations.

Errors in area terms. By linearity of scalar product and cross product or, equivalently, of determinant, noise-related error terms on area measures are straightforwardly obtained by developing $\mu_{\hat{\mathbf{u}}}^{(0)}(\hat{\tau}_l) - \mu_{\mathbf{u}}^{(0)}(\tau_l)$ with the formulas given in Property 1 of the paper. We write

$$\mu_{\hat{\mathbf{u}}}^{(0)}(\hat{\tau}_l) - \mu_{\mathbf{u}}^{(0)}(\tau_l) = \sum_{m=1}^3 \mathcal{L}_m^{(0)}(\tau_l; \mathbf{u}, \Delta \mathbf{x}; \boldsymbol{\varepsilon}, \boldsymbol{\xi}), \quad (1)$$

where $\mathcal{L}_m^{(0)}$ designates a sum of linear combination $\langle \cdot | \cdot \times \cdot \rangle$ of three terms among some \mathbf{u} , some difference between positions \mathbf{x} and m terms among the three terms are either a perturbation of position or a perturbation of normals. More precisely, we have:

$$\begin{aligned} \mathcal{L}_1^{(0)}(\tau_l; \mathbf{u}, \Delta \mathbf{x}; \boldsymbol{\varepsilon}, \boldsymbol{\xi}) &:= \frac{1}{2} \langle \bar{\xi}_l | (\mathbf{x}_{j_l} - \mathbf{x}_{i_l}) \times (\mathbf{x}_{k_l} - \mathbf{x}_{i_l}) \rangle + \frac{1}{2} \langle \bar{\mathbf{u}}_l | (\mathbf{x}_{j_l} - \mathbf{x}_{i_l}) \times \boldsymbol{\varepsilon}_{k_l} + (\mathbf{x}_{k_l} - \mathbf{x}_{j_l}) \times \boldsymbol{\varepsilon}_{i_l} + (\mathbf{x}_{i_l} - \mathbf{x}_{k_l}) \times \boldsymbol{\varepsilon}_{i_l} \rangle, \\ \mathcal{L}_2^{(0)}(\tau_l; \mathbf{u}, \Delta \mathbf{x}; \boldsymbol{\varepsilon}, \boldsymbol{\xi}) &:= \frac{1}{2} \langle \bar{\mathbf{u}}_l | (\boldsymbol{\varepsilon}_{j_l} - \boldsymbol{\varepsilon}_{i_l}) \times (\boldsymbol{\varepsilon}_{k_l} - \boldsymbol{\varepsilon}_{i_l}) \rangle + \frac{1}{2} \langle \bar{\xi}_l | (\mathbf{x}_{j_l} - \mathbf{x}_{i_l}) \times \boldsymbol{\varepsilon}_{k_l} + (\mathbf{x}_{k_l} - \mathbf{x}_{j_l}) \times \boldsymbol{\varepsilon}_{i_l} + (\mathbf{x}_{i_l} - \mathbf{x}_{k_l}) \times \boldsymbol{\varepsilon}_{i_l} \rangle, \\ \mathcal{L}_3^{(0)}(\tau_l; \mathbf{u}, \Delta \mathbf{x}; \boldsymbol{\varepsilon}, \boldsymbol{\xi}) &:= \frac{1}{2} \langle \bar{\xi}_l | (\boldsymbol{\varepsilon}_{j_l} - \boldsymbol{\varepsilon}_{i_l}) \times (\boldsymbol{\varepsilon}_{k_l} - \boldsymbol{\varepsilon}_{i_l}) \rangle. \end{aligned}$$

Errors in mean curvature measure terms. The error in curvature measure can also be written as:

$$\mu_{\hat{\mathbf{u}}}^{(1)}(\hat{\tau}_l) - \mu_{\mathbf{u}}^{(1)}(\tau_l) = \sum_{m=1}^3 \mathcal{L}_m^{(1)}(\tau_l; \mathbf{u}, \Delta \mathbf{x}; \boldsymbol{\varepsilon}, \boldsymbol{\xi}), \quad (2)$$

and noise-related error terms on mean curvature measures are also obtained as sum of linear combination $\langle \cdot | \cdot \times \cdot \rangle$:

$$\begin{aligned}\mathcal{L}_1^{(1)}(\tau_l; \mathbf{u}, \Delta \mathbf{x}; \boldsymbol{\varepsilon}, \xi) &:= \frac{1}{2} \langle \bar{\mathbf{u}}_l | (\mathbf{x}_{j_l} - \mathbf{x}_{i_l}) \times \xi_{k_l} + (\mathbf{x}_{k_l} - \mathbf{x}_{j_l}) \times \xi_{i_l} + (\mathbf{x}_{i_l} - \mathbf{x}_{k_l}) \times \xi_{j_l} \rangle \\ &\quad + \frac{1}{2} \langle \bar{\xi}_l | (\mathbf{x}_{j_l} - \mathbf{x}_{i_l}) \times \mathbf{u}_{k_l} + (\mathbf{x}_{k_l} - \mathbf{x}_{j_l}) \times \mathbf{u}_{i_l} + (\mathbf{x}_{i_l} - \mathbf{x}_{k_l}) \times \mathbf{u}_{j_l} \rangle \\ &\quad + \frac{1}{2} \langle \bar{\mathbf{u}}_l | \boldsymbol{\varepsilon}_{i_l} \times (\mathbf{u}_{j_l} - \mathbf{u}_{k_l}) + \boldsymbol{\varepsilon}_{j_l} \times (\mathbf{u}_{k_l} - \mathbf{u}_{i_l}) + \boldsymbol{\varepsilon}_{k_l} \times (\mathbf{u}_{i_l} - \mathbf{u}_{j_l}) \rangle, \\ \mathcal{L}_2^{(1)}(\tau_l; \mathbf{u}, \Delta \mathbf{x}; \boldsymbol{\varepsilon}, \xi) &:= \frac{1}{2} \langle \bar{\xi}_l | (\mathbf{x}_{j_l} - \mathbf{x}_{i_l}) \times \xi_{k_l} + (\mathbf{x}_{k_l} - \mathbf{x}_{j_l}) \times \xi_{i_l} + (\mathbf{x}_{i_l} - \mathbf{x}_{k_l}) \times \xi_{j_l} \rangle \\ &\quad + \frac{1}{2} \langle \bar{\mathbf{u}}_l | (\boldsymbol{\varepsilon}_{j_l} - \boldsymbol{\varepsilon}_{i_l}) \times \xi_{k_l} + (\boldsymbol{\varepsilon}_{k_l} - \boldsymbol{\varepsilon}_{j_l}) \times \xi_{i_l} + (\boldsymbol{\varepsilon}_{i_l} - \boldsymbol{\varepsilon}_{k_l}) \times \xi_{j_l} \rangle \\ &\quad + \frac{1}{2} \langle \bar{\xi}_l | \boldsymbol{\varepsilon}_{i_l} \times (\mathbf{u}_{j_l} - \mathbf{u}_{k_l}) + \boldsymbol{\varepsilon}_{j_l} \times (\mathbf{u}_{k_l} - \mathbf{u}_{i_l}) + \boldsymbol{\varepsilon}_{k_l} \times (\mathbf{u}_{i_l} - \mathbf{u}_{j_l}) \rangle, \\ \mathcal{L}_3^{(1)}(\tau_l; \mathbf{u}, \Delta \mathbf{x}; \boldsymbol{\varepsilon}, \xi) &:= \frac{1}{2} \langle \bar{\xi}_l | (\boldsymbol{\varepsilon}_{j_l} - \boldsymbol{\varepsilon}_{i_l}) \times \xi_{k_l} + (\boldsymbol{\varepsilon}_{k_l} - \boldsymbol{\varepsilon}_{j_l}) \times \xi_{i_l} + (\boldsymbol{\varepsilon}_{i_l} - \boldsymbol{\varepsilon}_{k_l}) \times \xi_{j_l} \rangle.\end{aligned}$$

Property of error laws.

Property 1 The error laws $\bar{Z}_L^{(0)}$ and $\bar{Z}_L^{(1)}$ have both null expectations. Their variance follows, for C and C' some constants:

$$\begin{aligned}\mathbb{V}[\bar{Z}_L^{(0)}] &\leq \frac{C}{L} \left((\sigma_\xi^2 \delta^2 + \sigma_\varepsilon^2) \delta^2 + \sigma_\varepsilon^2 \sigma_\xi^2 \delta^2 + \sigma_\varepsilon^4 (1 + \sigma_\xi^2) \right) \\ \mathbb{V}[\bar{Z}_L^{(1)}] &\leq \frac{C'}{L} \left(\sigma_\xi^2 \delta^2 + \sigma_\varepsilon^2 + \sigma_\varepsilon^2 \sigma_\xi^2 + \sigma_\xi^4 \delta^2 + \sigma_\varepsilon^2 \sigma_\xi^4 \right).\end{aligned}$$

Proof First, to prove that the error laws $\bar{Z}_L^{(0)}$ and $\bar{Z}_L^{(1)}$ have both null expectations, it suffices to examine the expectation of each term $\mathcal{L}_m^{(r)}(\tau_l; \mathbf{u}, \Delta \mathbf{x}; \boldsymbol{\varepsilon}, \xi)$. Either there is an isolated normal perturbation ξ , or there is an average of independent normal perturbations $\bar{\xi}$ or even an isolated position perturbation $\boldsymbol{\varepsilon}$. All those cases imply trivially a null expectation for this term. The only trickier cases are terms of the form $\langle \cdot | (\boldsymbol{\varepsilon}_{j_l} - \boldsymbol{\varepsilon}_{i_l}) \times (\boldsymbol{\varepsilon}_{k_l} - \boldsymbol{\varepsilon}_{i_l}) \rangle$. But developing them leads to independent terms $\boldsymbol{\varepsilon}$, while the non-independent term $\langle \cdot | (\boldsymbol{\varepsilon}_{i_l} \times \boldsymbol{\varepsilon}_{i_l}) \rangle$ is trivially null. So the two laws have null expectation.

Now let us prove the bounds on their variance. From the definition of $\bar{Z}_L^{(0)}$, we get that $\bar{Z}_L^{(0)} = \frac{1}{L} \sum_{l=1}^L (\mu_{\bar{\mathbf{u}}}^{(0)}(\hat{\tau}_l) - \mu_{\bar{\mathbf{u}}}^{(0)}(\tau_l))$. Since the triangles are independent, we get that $\mathbb{V}[\bar{Z}_L^{(0)}] = \frac{1}{L} \mathbb{V}[\mu_{\bar{\mathbf{u}}}^{(0)}(\hat{\tau}_l) - \mu_{\bar{\mathbf{u}}}^{(0)}(\tau_l)]$, for any l . Let us bound the latter term. From (1) we have

$$\mathbb{V}[\mu_{\bar{\mathbf{u}}}^{(0)}(\hat{\tau}_l) - \mu_{\bar{\mathbf{u}}}^{(0)}(\tau_l)] = \sum_{m=1}^3 \mathbb{V}[\mathcal{L}_m^{(0)}(\tau_l; \mathbf{u}, \Delta \mathbf{x}; \boldsymbol{\varepsilon}, \xi)] + 2 \sum_{m=1}^3 \sum_{n=1}^{m-1} \mathbb{Cov}[\mathcal{L}_m^{(0)}(\tau_l; \mathbf{u}, \Delta \mathbf{x}; \boldsymbol{\varepsilon}, \xi), \mathcal{L}_n^{(0)}(\tau_l; \mathbf{u}, \Delta \mathbf{x}; \boldsymbol{\varepsilon}, \xi)].$$

Since δ bounds the distance between points $(\mathbf{x}_{i_l}, \mathbf{x}_{j_l}, \mathbf{x}_{k_l})$, $\bar{\mathbf{u}}_l$ is a unit vector, and since

- for all (k, l) the random variables ξ_k and $\boldsymbol{\varepsilon}_l$ are independent,
- for all $k \neq l$ $\boldsymbol{\varepsilon}_k$ is independent from $\boldsymbol{\varepsilon}_l$
- for all $i \neq j$ $\mathbb{Cov}[\boldsymbol{\varepsilon}_i(i), \boldsymbol{\varepsilon}_l(j)] = 0$,
- for a random variable X , $\mathbb{V}[X] = \mathbb{E}[X^2]$ when $\mathbb{E}[X] = 0$,

we get

$$\begin{aligned}\mathbb{V}[\mathcal{L}_1^{(0)}(\tau_l; \mathbf{u}, \Delta \mathbf{x}; \boldsymbol{\varepsilon}, \xi)] &\leq C(\sigma_\xi^2 \delta^4 + \sigma_\varepsilon^2 \delta^2), \\ \mathbb{V}[\mathcal{L}_2^{(0)}(\tau_l; \mathbf{u}, \Delta \mathbf{x}; \boldsymbol{\varepsilon}, \xi)] &\leq C(\sigma_\varepsilon^4 + \sigma_\varepsilon^2 \sigma_\xi^2 \delta^2), \\ \mathbb{V}[\mathcal{L}_3^{(0)}(\tau_l; \mathbf{u}, \Delta \mathbf{x}; \boldsymbol{\varepsilon}, \xi)] &\leq C(\sigma_\varepsilon^4 \sigma_\xi^2).\end{aligned}$$

The assumptions on the random variables ξ and $\boldsymbol{\varepsilon}$ give that for all $m \neq n$ it holds

$$\mathbb{Cov}[\mathcal{L}_m^{(0)}(\tau_l; \mathbf{u}, \Delta \mathbf{x}; \boldsymbol{\varepsilon}, \xi), \mathcal{L}_n^{(0)}(\tau_l; \mathbf{u}, \Delta \mathbf{x}; \boldsymbol{\varepsilon}, \xi)] = 0$$

and the first result follows. As for $\bar{Z}_L^{(1)}$, we get that $\mathbb{V}[\bar{Z}_L^{(1)}] = \frac{1}{L} \mathbb{V}[\mu_{\bar{\mathbf{u}}}^{(1)}(\hat{\tau}_l) - \mu_{\bar{\mathbf{u}}}^{(1)}(\tau_l)]$, for any l . Let us bound the latter term. From (2), we have

$$\mathbb{V}[\mu_{\bar{\mathbf{u}}}^{(1)}(\hat{\tau}_l) - \mu_{\bar{\mathbf{u}}}^{(1)}(\tau_l)] = \sum_{m=1}^3 \mathbb{V}[\mathcal{L}_m^{(1)}(\tau_l; \mathbf{u}, \Delta \mathbf{x}; \boldsymbol{\varepsilon}, \xi)] + 2 \sum_{m=1}^3 \sum_{n=1}^{m-1} \mathbb{Cov}[\mathcal{L}_m^{(1)}(\tau_l; \mathbf{u}, \Delta \mathbf{x}; \boldsymbol{\varepsilon}, \xi), \mathcal{L}_n^{(1)}(\tau_l; \mathbf{u}, \Delta \mathbf{x}; \boldsymbol{\varepsilon}, \xi)].$$

Using the same arguments as before yields

$$\begin{aligned}\mathbb{V}\left[\mathcal{L}_1^{(1)}(\tau_l; \mathbf{u}, \Delta \mathbf{x}; \varepsilon, \xi)\right] &\leq C(\sigma_\xi^2 \delta^2 + \sigma_\varepsilon^2), \\ \mathbb{V}\left[\mathcal{L}_2^{(1)}(\tau_l; \mathbf{u}, \Delta \mathbf{x}; \varepsilon, \xi)\right] &\leq C(\sigma_\xi^4 \delta^2 + \sigma_\varepsilon^2 \sigma_\xi^2), \\ \mathbb{V}\left[\mathcal{L}_3^{(1)}(\tau_l; \mathbf{u}, \Delta \mathbf{x}; \varepsilon, \xi)\right] &\leq C(\sigma_\varepsilon^2 \sigma_\xi^4),\end{aligned}$$

and the covariance terms are null. \square

2. Discussion on CNC-Avg-Hexagram

One could wonder why the CNC-Avg-Hexagram variant produces such accurate results while being apparently quite far from the hypotheses of stability Theorem 1 and error laws (Property 2). The answer lies in the linearity of all interpolated curvature measure formula. Since the positions $\hat{\mathbf{y}}_j$ and the normals $\hat{\mathbf{v}}_j$ are averaged, they can be replaced in each linear combination $\langle \cdot | \cdot \times \cdot \rangle$ by these averages. For instance, to simplify the reasoning, if each region j had the same number of vertices, say k , each term $\langle \cdot | \cdot \times \cdot \rangle$ of any measure formula can be developed as k^3 different terms. It is as if we are testing all possible combinations of points/normals between the three regions of each triangle. But instead of computing k^3 triangles (as CNC-Uniform is doing) we only compute one triangle. Even better, since the points are taken in well-chosen regions, all these possible triangle combinations are much more equilateral than a uniform random generation. Finally, if the number of triangles is not the same within the three regions, the reasoning still holds since this situation induces *weighted* combinations of triangles. Note that this method works solely because curvature measures are normalized by the corresponding area measures, with the same weights involved.

3. Experimental evaluation

3.1. Extraction of principal directions

Although we did not showcase it in the main paper, our method also provides accurate estimates of principal directions. We could also achieve the same kind of stability theorem for principal directions that we did with mean curvature. It would require to use matrix perturbation theory results, using Davis-Kahan theorem [Dav63] and Lidskii-Weyl inequality. We display on Figure 1 an example of principal directions computation on real scanned data.

3.2. Influence of the neighborhood size

Figure 2 completes Figure 5 of the main paper and shows how different curvature estimators behave on perfect and noisy data for the `torus` shape for $K = 50$. Figures 3 and 4 present mean and gaussian curvature results on the `goursat` and `torus` shape when considering a larger neighborhood, i.e. $K = 200$ neighbors (parameters are given in the figures caption). These figures must be compared with Figure 4 in the main document and Figure 2 where only 50 neighbors have been considered. As expected, when K increases, JetFitting and ASO results get improved. For big K , the accuracy of ASO is comparable to our method.

3.3. Point clouds with non-uniform densities

Figures 5, 6, 7 and 8 show results on non-uniform density point clouds, illustrating the stability of our approach. Finally, 9 and 10 illustrate curvature results on strongly anisotropic point clouds, generated using a LIDAR-like sampling of the `goursat` and `torus` surfaces. Note that normal vectors of perfect data are obtained from the respective implicit surfaces (perturbed using the Gaussian noise model for the noisy data experiments).

References

- [CP05] CAZALS F., POUGET M.: Estimating differential quantities using polynomial fitting of osculating jets. *Computer Aided Geometric Design* 22, 2 (2005), 121 – 146. doi:<https://doi.org/10.1016/j.cagd.2004.09.004>. 5, 6, 7, 8, 9, 10, 11, 12, 13
- [Dav63] DAVIS C.: The rotation of eigenvectors by a perturbation. *Journal of Mathematical Analysis and Applications* 6, 2 (1963), 159 – 173. URL: <http://www.sciencedirect.com/science/article/pii/0022247X63900015>, doi:[http://dx.doi.org/10.1016/0022-247X\(63\)90001-5](http://dx.doi.org/10.1016/0022-247X(63)90001-5). 3
- [LCBM21] LEJEMBLE T., COEURJOLLY D., BARTHE L., MELLADO N.: Stable and efficient differential estimators on oriented point clouds. *Computer Graphics Forum (Proceedings of Symposium on Geometry Processing)* 40, 5 (July 2021). doi:[10.1111/cgfm.14368](https://doi.org/10.1111/cgfm.14368). 5, 6, 7, 8, 9, 10, 11, 12, 13

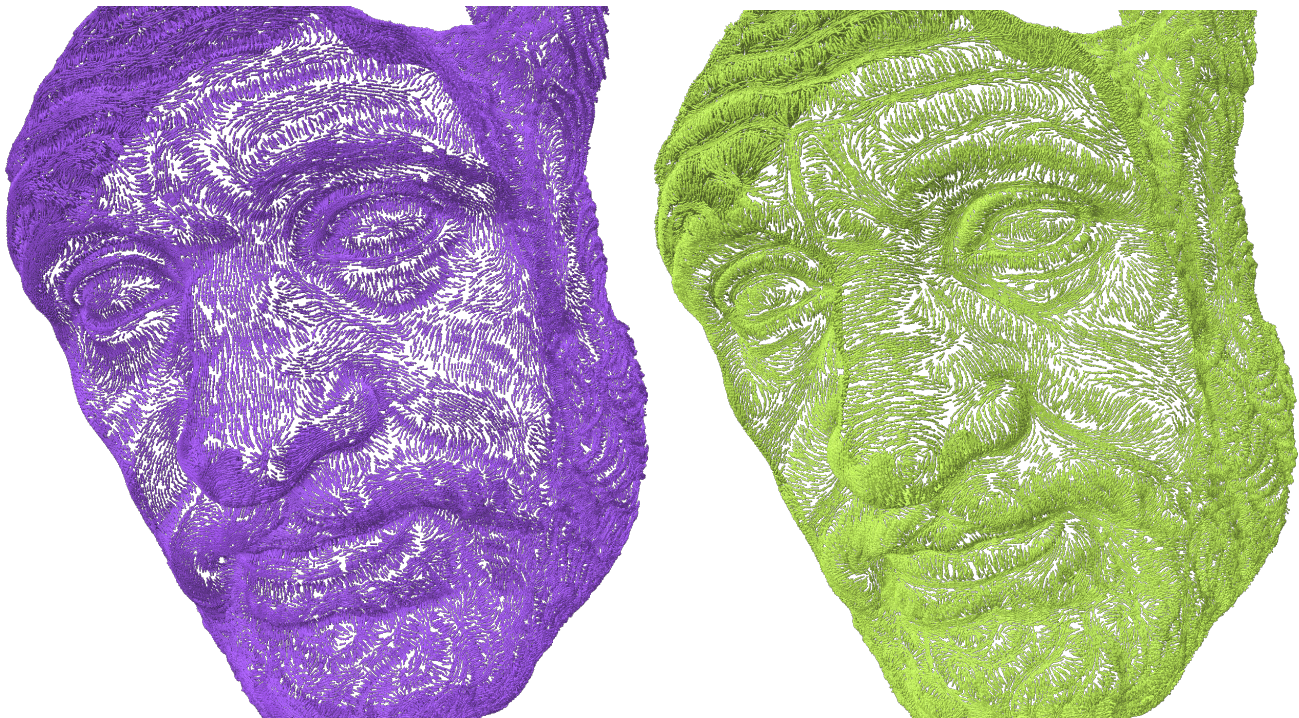


Figure 1: First and second principal directions on scanned data (from <https://threedscans.com>), using CNC-Avg-Hexagram with $K = 50$, objects is composed of 499500 points.

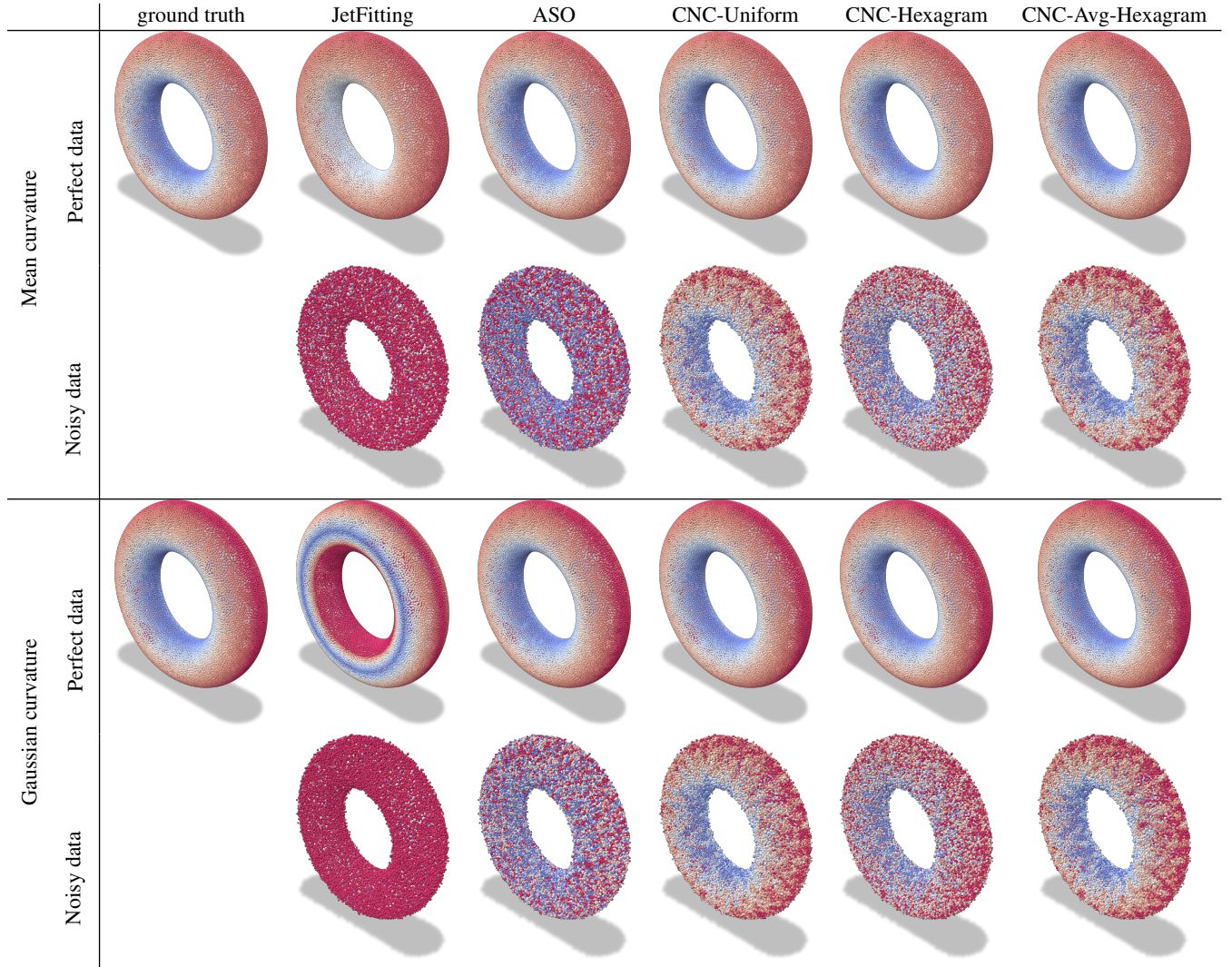


Figure 2: Visual comparisons for $K = 50$ on point clouds sampling the zero level set surface of `torus` ($N = 25000$), without or with noise ($\sigma_e = \sigma_\xi = 0.1$). We compare JetFitting [CP05], ASO [LCBM21], CNC-Uniform ($L = 100$), CNC-Hexagram and CNC-Avg-Hexagram. The colormap range for mean curvature (resp. Gaussian curvature) values is $[0.125, 0.32]$ (resp. $[-0.125, 0.0625]$).

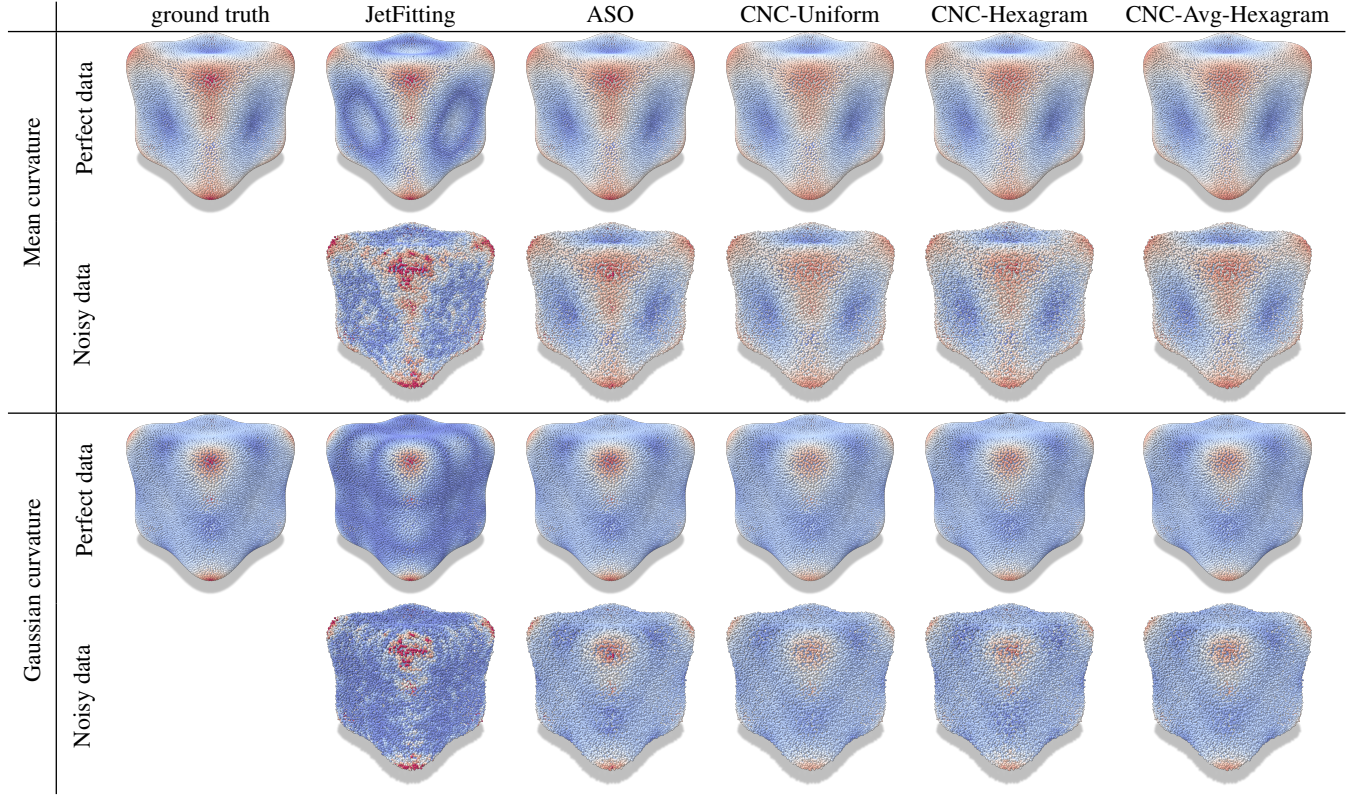


Figure 3: Visual comparisons for $K = 200$ on point clouds sampling the zero level set surface of *goursat* ($N = 25000$), without or with noise ($\sigma_\epsilon = \sigma_\xi = 0.1$). We compare JetFitting [CP05], ASO [LCBM21], CNC-Uniform ($L = 200$), CNC-Hexagram and CNC-Avg-Hexagram. The colormap range for mean curvature (resp. Gaussian curvature) values is $[-0.107, 0.345]$ (resp. $[-0.034, 0.119]$).

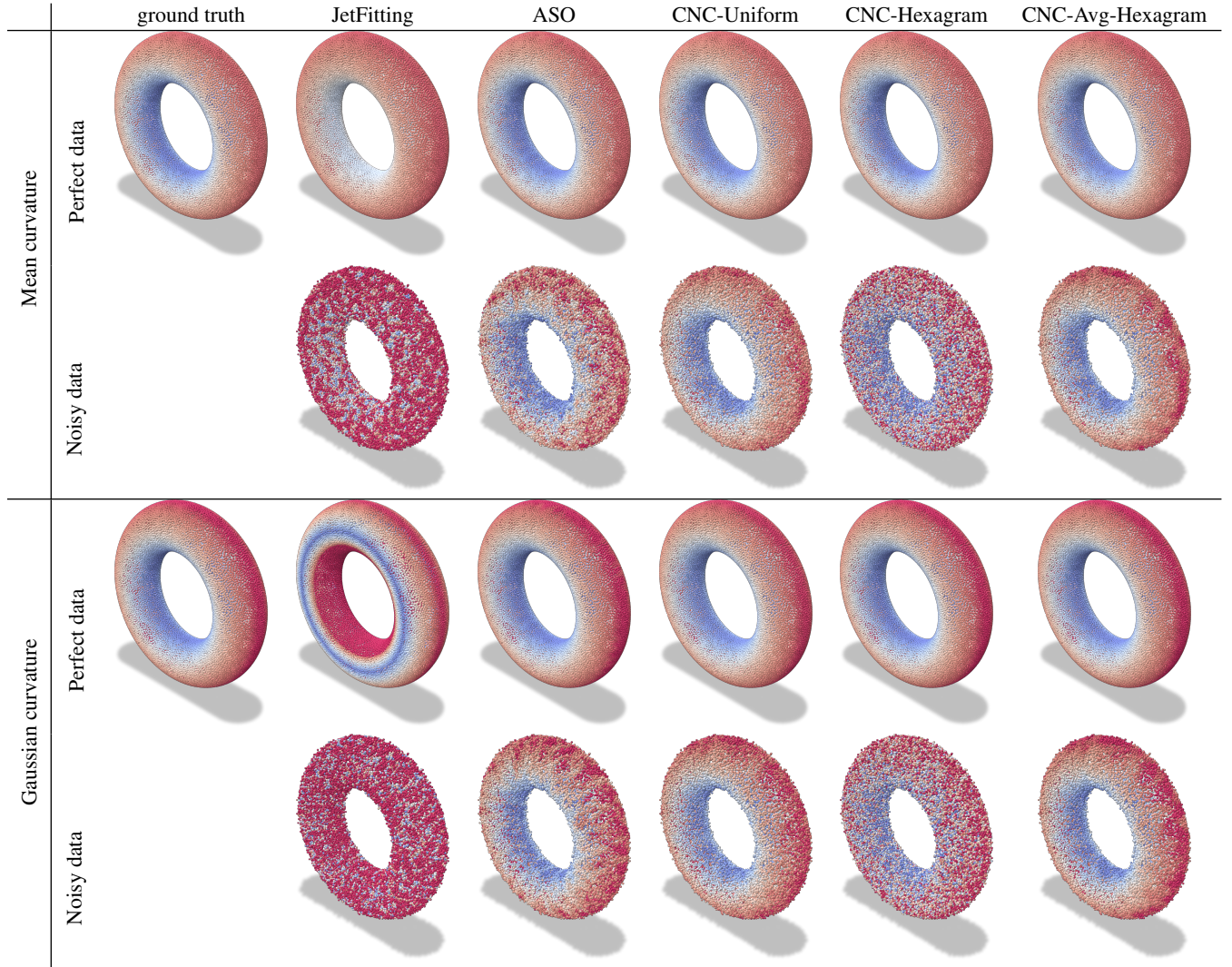


Figure 4: Visual comparisons for $K = 200$ on point clouds sampling the zero level set surface of `torus` ($N = 25000$), without or with noise ($\sigma_e = \sigma_\xi = 0.1$). We compare JetFitting [CP05], ASO [LCBM21], CNC-Uniform ($L = 200$), CNC-Hexagram and CNC-Avg-Hexagram. The colormap range for mean curvature (resp. Gaussian curvature) values is $[0.125, 0.32]$ (resp. $[-0.125, 0.0625]$).

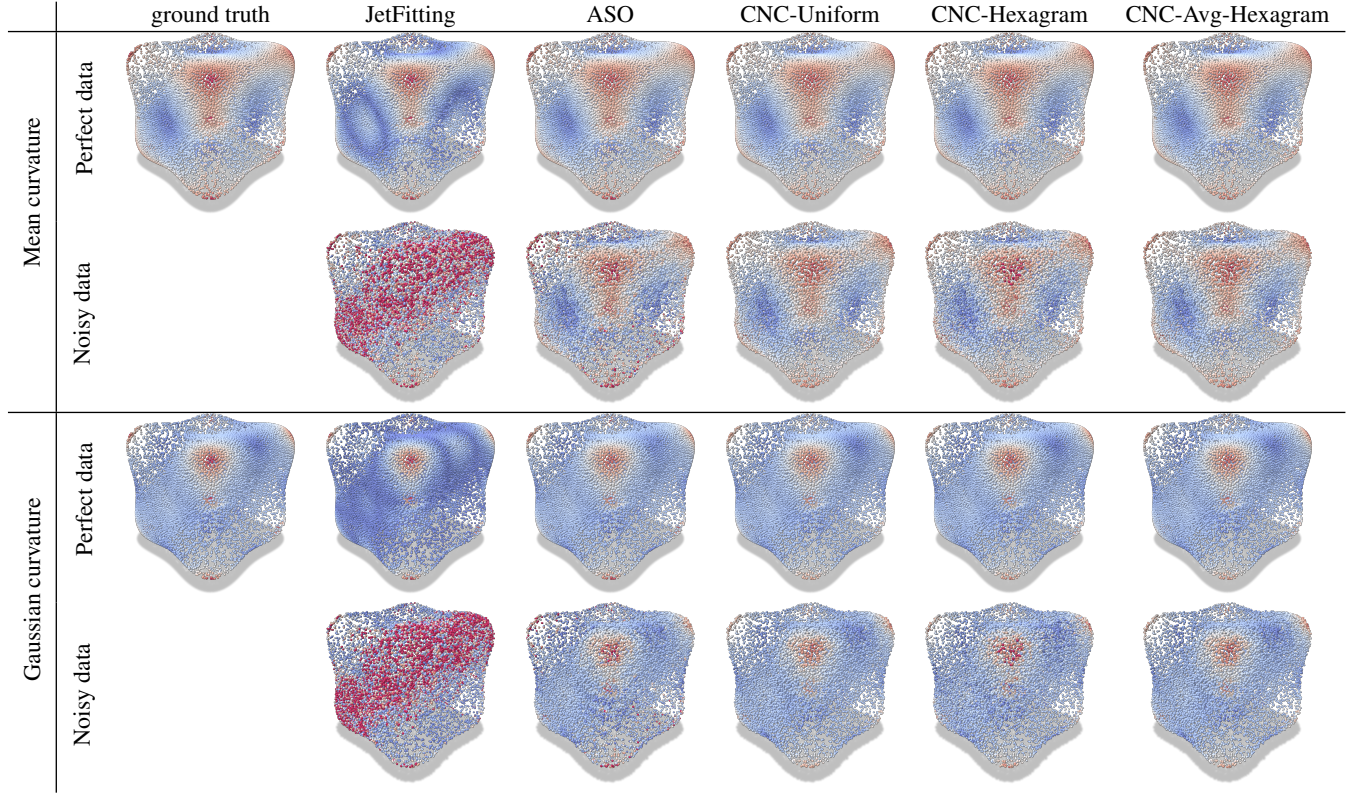


Figure 5: Visual comparisons for $K = 50$ on point clouds with non-uniform density sampling the zero level set surface of *goursat* ($N = 25000$), without or with noise ($\sigma_\epsilon = \sigma_\xi = 0.1$). We compare JetFitting [CP05], ASO [LCBM21], CNC-Uniform ($L = 200$), CNC-Hexagram and CNC-Avg-Hexagram. The colormap range for mean curvature (resp. Gaussian curvature) values is $[-0.107, 0.345]$ (resp. $[-0.034, 0.119]$).

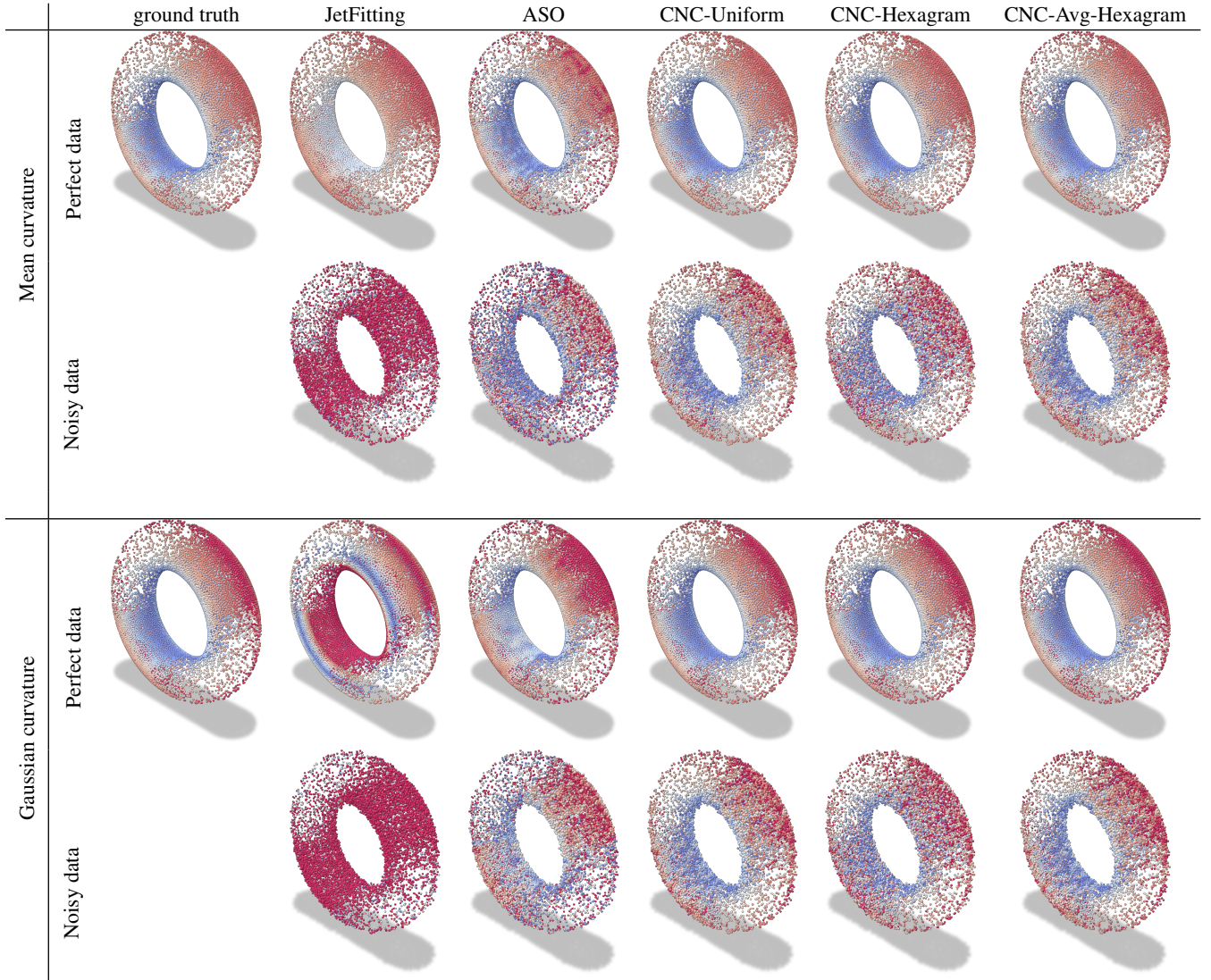


Figure 6: Visual comparisons for $K = 50$ on point clouds with non-uniform density sampling the zero level set surface of torus ($N = 25000$), without or with noise ($\sigma_\varepsilon = \sigma_\xi = 0.1$). We compare JetFitting [CP05], ASO [LCBM21], CNC-Uniform ($L = 200$), CNC-Hexagram and CNC-Avg-Hexagram. The colormap range for mean curvature (resp. Gaussian curvature) values is $[0.125, 0.32]$ (resp. $[-0.125, 0.0625]$).

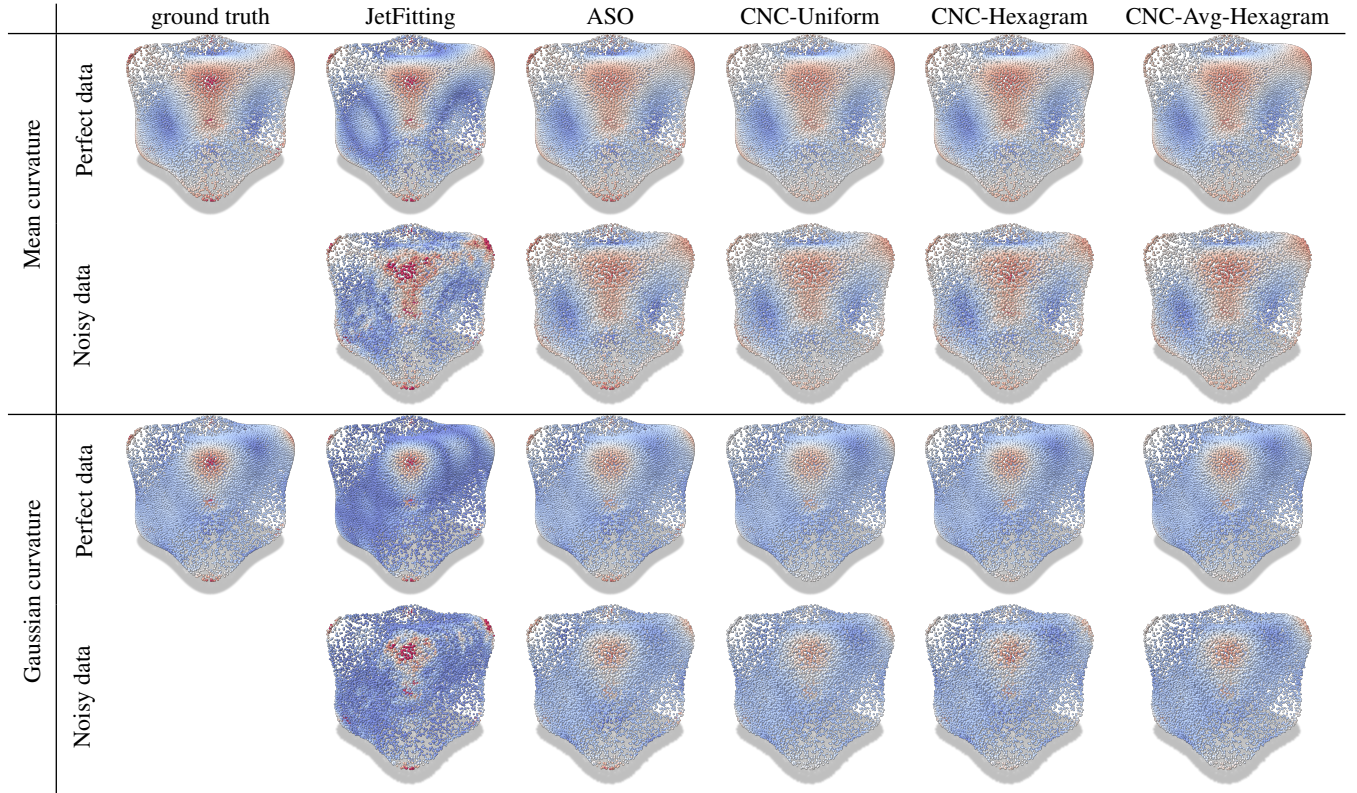


Figure 7: Visual comparisons for $K = 200$ on point clouds with non-uniform density sampling the zero level set surface of *goursat* ($N = 25000$), without or with noise ($\sigma_\epsilon = \sigma_\xi = 0.1$). We compare JetFitting [CP05], ASO [LCBM21], CNC-Uniform ($L = 200$), CNC-Hexagram and CNC-Avg-Hexagram. The colormap range for mean curvature (resp. Gaussian curvature) values is $[-0.107, 0.345]$ (resp. $[-0.034, 0.119]$).

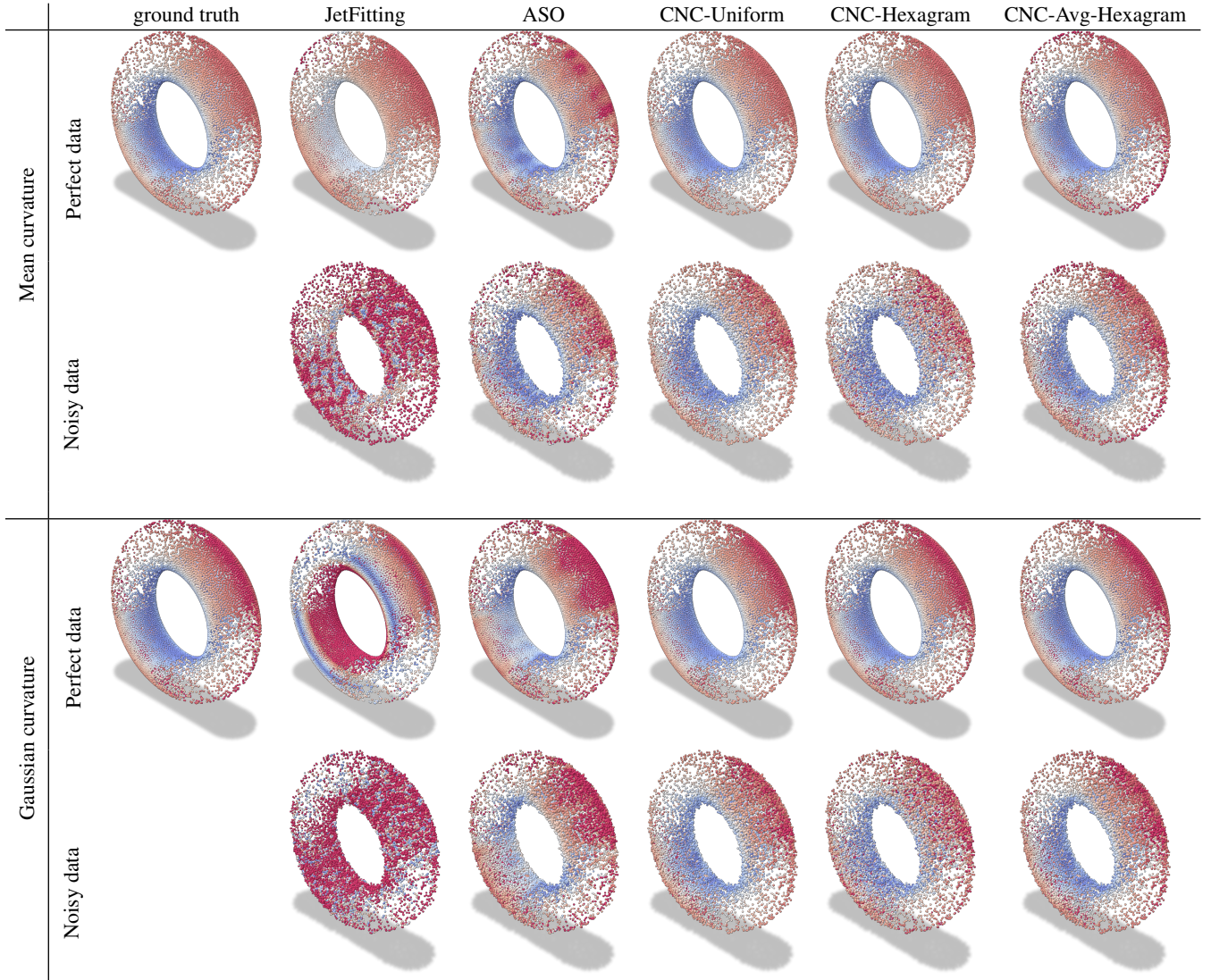


Figure 8: Visual comparisons for $K = 200$ on point clouds with non-uniform density sampling the zero level set surface of torus ($N = 25000$), without or with noise ($\sigma_\epsilon = \sigma_\xi = 0.1$). We compare JetFitting [CP05], ASO [LCBM21], CNC-Uniform ($L = 200$), CNC-Hexagram and CNC-Avg-Hexagram. The colormap range for mean curvature (resp. Gaussian curvature) values is $[0.125, 0.32]$ (resp. $[-0.125, 0.0625]$).

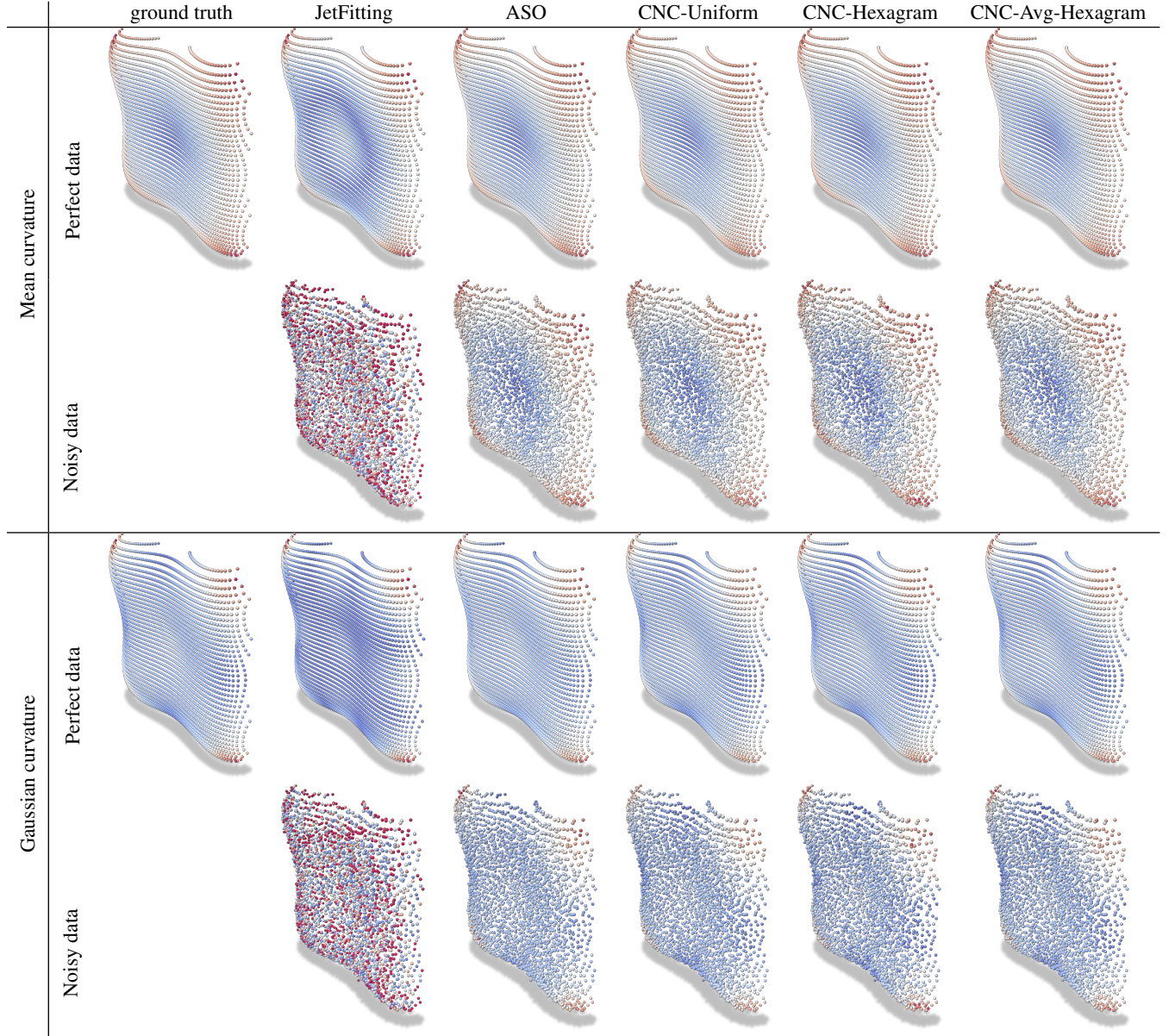


Figure 9: Visual comparisons for $K = 50$ on point clouds mimicking LiDAR density sampling the zero level set surface of *goursat* ($N = 2947$), without or with noise ($\sigma_\epsilon = \sigma_\xi = 0.1$). We compare JetFitting [CP05], ASO [LCBM21], CNC-Uniform ($L = 200$), CNC-Hexagram and CNC-Avg-Hexagram. The colormap range for mean curvature (resp. Gaussian curvature) values is $[-0.107, 0.345]$ (resp. $[-0.034, 0.119]$).

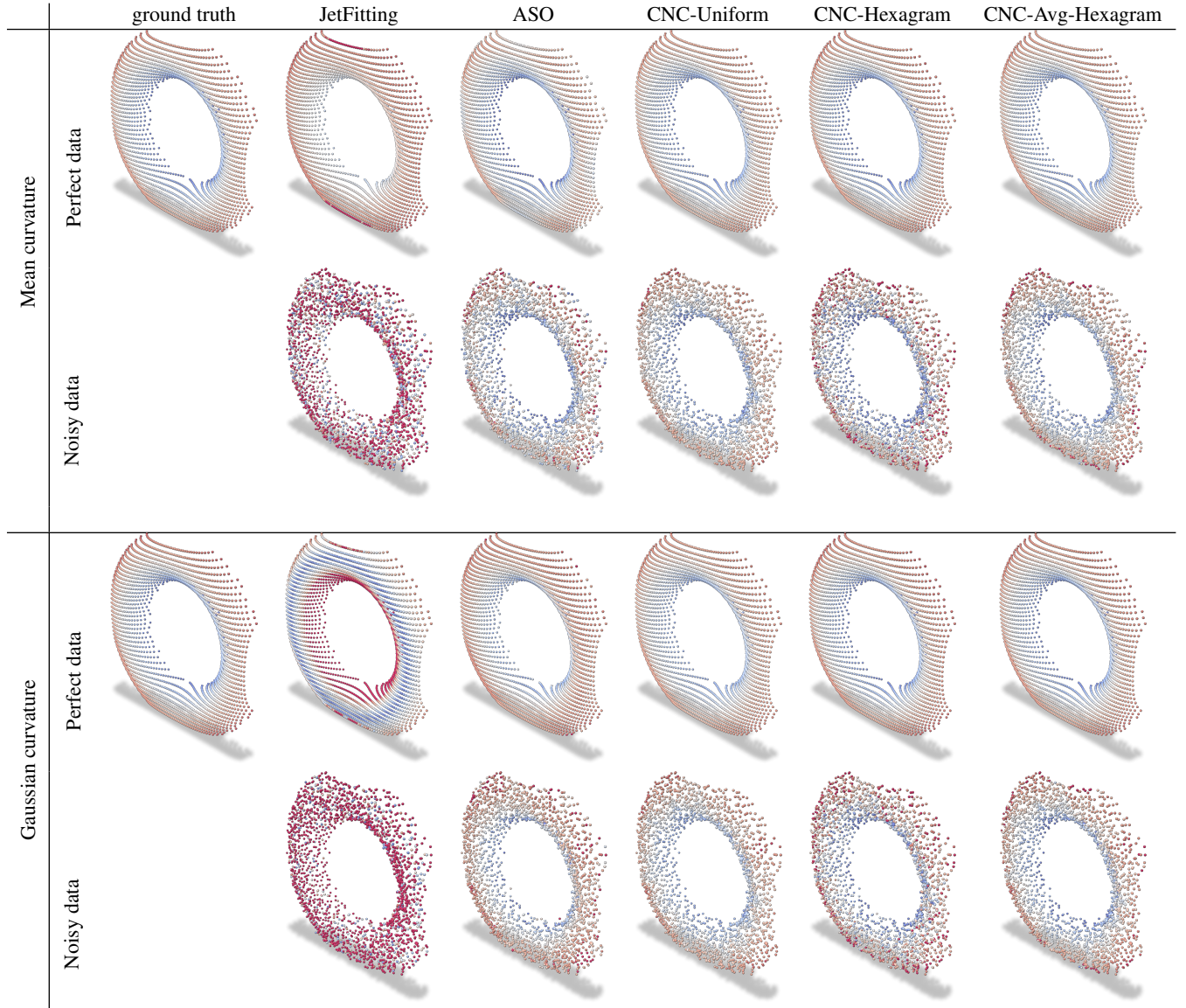


Figure 10: Visual comparisons for $K = 50$ on point clouds mimicking LiDAR density sampling the zero level set surface of torus ($N = 2086$), without or with noise ($\sigma_{\epsilon} = \sigma_{\xi} = 0.1$). We compare JetFitting [CP05], ASO [LCBM21], CNC-Uniform ($L = 200$), CNC-Hexagram and CNC-Avg-Hexagram. The colormap range for mean curvature (resp. Gaussian curvature) values is $[0.125, 0.32]$ (resp. $[-0.125, 0.0625]$).